Multiresolution quantum chemistry: Basic theory and initial applications

Robert J. Harrison, George I. Fann, Takeshi Yanai, and Zhengting Gan
Oak Ridge National Laboratory, Oak Ridge, Tennessee 37831

Gregory Beylkin
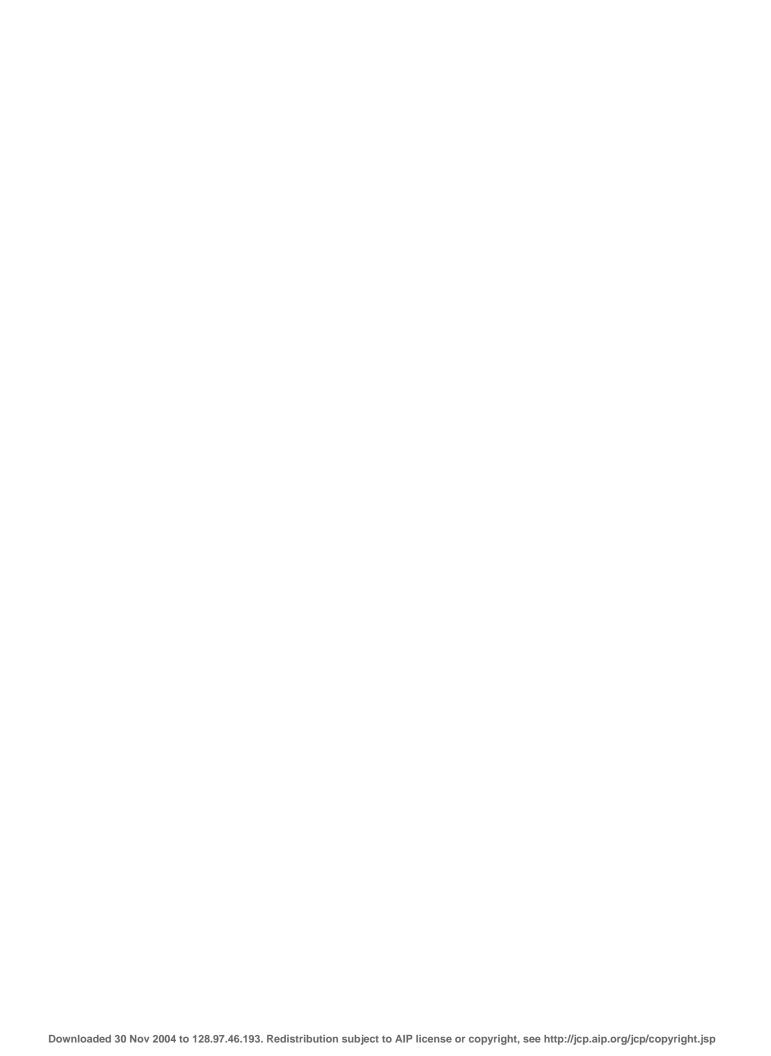*Department of Applied Mathematics, University of Colorado at Boulder, Boulder, Colorado 80309-0526*

We describe a multiresolution solver for the all-electron local density approximation Kohn-Sham equations for general polyatomic molecules. The resulting solutions are obtained to a user-specified precision and the computational cost of applying all operators scales linearly with the number of parameters. The construction and use of separated forms for operators here, the Green's functions for the Poisson and bound-state Helmholtz equations) enable practical computation in three and higher dimensions. Initial applications include the alkali-earth atoms down to strontium and the water and benzene molecules. © *2004 American Institute of Physics.* [DOI: 10.1063/1.1791051]

I. INTRODUCTION

We describe a multiresolution solver for the all-electron local density approximation LDA) Kohn-Sham[1] equations for molecules. The objective of this work is to provide a practical approach for computation on general polyatomic systems without basis set error and with the computational cost of applying all operators scaling linearly with the number of parameters. Besides using a multiresolution approach, a critical step in attaining this objective has been the development of separable representations for kernels of Green's functions.[2] We describe a prototype, orbital-based implementation with test application to closed-shell systems including the alkali-earth atoms down to strontium, and the water and benzene molecules. We consider that a demonstration of a practical approach for solution of one-electron methods is an essential precursor to direct numerical solution of two- and many-electron problems.

With only a few notable exceptions,[3,4] mainstream molecular quantum chemistry is performed with the linear combination of atomic orbitals LCAO) approximation most commonly using atom-centered Gaussian functions. These methods date back 50 years to the work of Roothaan,[5,6] Hall,[7] and Boys,[8] and many of the successes of modern

where s_l is a scalar, $s_1 \geqslant$ fl $\geqslant s_M > 0$, and $K_i^l(x_{j_i}, x_{j'_i})$ are kernels of normalized norm one) operators $\mathbb{T}_i^l$ in dimension $d = 1$. We require the error to be less than , namely,

$$\| \mathbb{T} - \sum_{l=1}^{M} s_l \mathbb{T}_1^l \otimes \mathbb{T}_2^l \otimes \text{fl} \otimes \mathbb{T}_d^l \| < .$$

2)

We call the scalars s_l separation values and the integer M the

We then use an algorithm for constructing a nearly optimal representation using Ref. 38, where the authors extend the approach in Ref. 39. As a result, we find the generalized Gaussian nodes and weights such that

$$\frac{1}{r} - \sum_{m=1}^{M} {}_m e^{-p_m r^2} \leqslant \frac{}{r}, \qquad (11)$$

where   is the required maximum relative error within the range and where the number of terms, M, is nearly optimal. The optimization procedure in Ref. 38 also allows us to obtain an approximation

$$\frac{1}{r} - \sum_{m=1}^{M} {}_m e^{-p_m r^2} \leqslant \frac{}{r^2}, \qquad (12)$$

which is sufficient to obtain Eq. 9) and requires fewer terms.

The third step in obtaning Eq. 9) is to substitute the approximation in Eq. 11) or 12) into Eq. 8) and compute one-dimensional integrals. A detailed derivation of these representations will appear separately.[40]

For instance, a 52-term representation was constructed to obtain a relative precision of 10^{-8} in the interval $[10^{-5}, 1]$ using Eq. 11). The representation obtained using the trapezoidal rule in Eq. 10) used 300+ terms, which may be partially reduced through elementary methods.[37] The optimal representations was then formed using Ref. 38, yielding 52 terms for the relative accuracy displayed in Fig. 1.

For >0, the kernel G in Eq. 3) is not homogeneous, so that the approximation should be constructed for each scale separately which will yield a compact representation of the matrix elements [see Eq. 5)] rather than of the kernel as a whole. Although this is clearly the most efficient approach, details of which we will present in a sequel, in the prototype code we used an expansion that spans all length scales. To generate the separated representation of G ,   0, we use instead of Eq. 10) the integral

$$\frac{e^{-\ r}}{r} = \frac{2}{\sqrt{}} \int_{-\infty}^{\infty} e^{-r^2 e^{2s} - \ ^2 e^{-2s} + s} ds. \qquad (13)$$

Due to the superexponential decay at both ends of the range, the trapezoidal rule may be directly applied to this integral to obtain the desired separated representation.[37] In our computations with G , we select the range of validity to include $[0.001/(LZ_{max}), 1.0]$, where Z_{max} is the maximum nuclear charge and L is the simulation cell size.

We note that for isotropic kernels, it is sufficient to compute the transition matrix elements for positive translations only. Values for negative translations are obtained using symmetries of the basis functions ${}_i(x) = (-1)^i \ {}_i(1-x)$. The one-dimensional 1D) transition matrix elements are computed and a singular value decomposition is performed for these matrices. Away from the singularity, the matrices have very low operator rank.

When applying the operator, a test is performed to see if it is more efficient to use a low-operator-rank form. In 1D, the break-even point is an operator rank less than half the matrix dimension. In 3D, if the transformations are done in order of increasing rank, the break-even ratios are about 3/4, 2/3, and 1/2 for the first, second, and third transformations, respectively.

Efficient application of the separated kernel requires screening based upon both the magnitude of the coefficients of the source function and the coefficients of the nonstandard form of the three-dimensional operator. We currently estimate the l^2 norm of each block of the operator using the power method, namely, the rapidly convergent iteration $|A|_2 = \lim_{n \to \infty} \sqrt{x_n / x_{n-1}}$, where $x_n = A^t A x_{n-1}$. Typically, two to four iterations provide more than one digit precision starting from a random initial guess.

III. KOHN-SHAM EQUATIONS

The nonlinear Kohn-Sham equations [e.g., Eqs. 7.2.7-9

nonlocal exchange potential [Eq. 2.5.12) in Ref. 1]. Implementation of gradient-corrected functionals, Hartree–Fock exchange, and hybrid potentials will be discussed in future publications.

The eigenvalues ϵ_i are also referred to as the orbital energies and will be negative for the occupied orbitals. The asymptotic form of the LDA occupied orbitals is obtained by substituting the form $r \exp{-\alpha}$
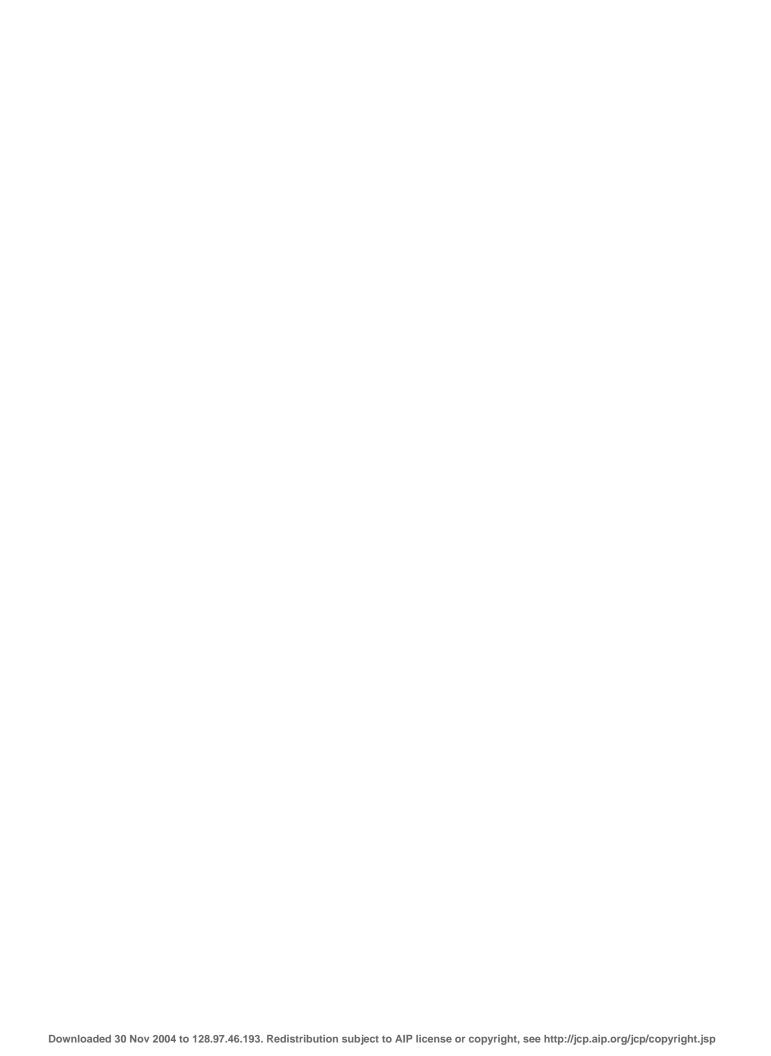
IV. ANALYTIC ENERGY DERIVATIVES

Derivatives of the variational Hartree–Fock or DFT energy with respect to the nuclear coordinates or any parameter in the external potential) are straightforwardly evaluated since the Hellman–Feynman theorem is obeyed up to the truncation threshold:

$$\frac{\partial E}{\partial q} = \frac{\partial V}{}$$

essary work is done processing matrices that are currently treated as dense and/or full rank. Odd orders are more efficient due to the superior error in derivatives.[14]

At each threshold   )

The H_2 molecule bond length 1.4 bohrs) was also used to examine the convergence behavior for iteration of the integral equation with and without use of the subspace information, and with and without the multiscale solution. All calculations started from the STO-3G orbital generated at a bond length of 2 bohrs. Simple iteration of the integral equation, updating the eigenvalue according to Eq. 30), using a multiwavelet of order $k=9$ and a truncation threshold of 10^{-7}, converged to a residual norm of 10^{-6} in ten iterations. Use of the iterative subspace information[47] to accelerate convergence reduces the number of iterations. For many-electron systems, this is essential for reliable convergence. Repeating these two calculations with the multiscale solver Sec. VI) requires a few more iterations overall, but requires only one iteration at the most accurate, and most expensive, threshold. Calculations at successive resolutions are approximately twofold to fourfold more expensive.
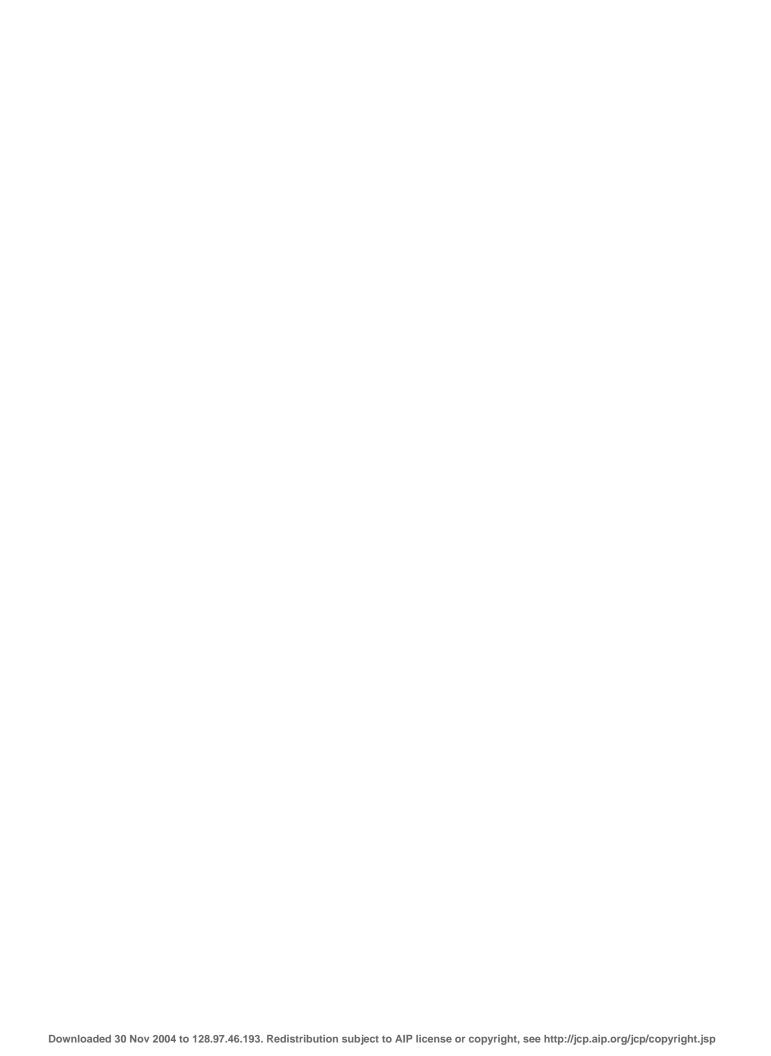
C. LDA calculations on atoms

We have implemented the local density approximation[1] LDA; the Dirac–Slater exchange potential with the VWN-5 correlation potential[41]) for closed shell systems. In order to verify the implementation and to explore possible issues with calculations on many-electron atoms, we performed calculations on the neutral atoms He, Be, Mg, Ca, and Sr. The results agree with the atomic data from the NIST database,[57] which are reported to six decimal places in atomic units.

Figure 3 displays a radial plot of the strontium s orbitals. The correct asymptotic decay Sec. III) is observed for each orbital until the truncation threshold is encountered. Previously, as described in Sec. VI, for all solution thresholds we employed diagonalization within the occupied space to incorporate the effects of deflation. Since the integral and differential forms of the LDA equations are only consistent up to the truncation threshold, diagonalization inevitably mixed the orbitals, resulting in less satisfactory asymptotic forms. The LDA equations were still being solved to the desired precision and the energy was correct. However, since the diagonalization does not significantly accelerate convergence once the eigenfunctions are identified to low precision, and to avoid mixing the final eigenfunctions of the integral equation, we presently only diagonalize in the occupied subspace with the initial solution threshold. This was how displayed orbitals were obtained.

D. LDA calculations on polyatomic molecules

LDA calculations were performed upon water and benzene near their equilibrium geomet7268.7(g-3.8(sfor-)]Ds0LDAT)6(cnd).2

populations can be readily accomplished by projection into a minimum atomic basis.[58]

The quantum chemical algorithms are written at a very high level in terms of operators and functions. This should be compared with the conventional approach in atomic bases which manipulates explicitly indexed, sparse, multidimensional arrays of matrix elements one- and two-electron integrals). This has led to the very rapid and compact implementation of energies, analytic derivatives, and linear response

[45] W. Hehre, R. Stewart, and J. Pople, J. Chem. Phys. **51**, 2657 1969).

[46] R. Kendall, E. Apra, D. Bernholdt *et al.*, Comput. Phys. Commun. **128**, 260 2000).

[47] R. J. Harrison, J. Comput. Chem. **25**, 328 2004).

[48] P. Pulay, Chem. Phys. Lett. **73**, 393 1980).

[49] See http://www.python.org

[50] See http://www.swig.org

[51] G. Beylkin and J. M. Keiser, J. Comput. Phys. **132**, 233 1997).

[52] See http://www.opendx.org

[53] B. Alpert, Ph.D. thesis, Yale University, 1990.

[54] T. Koga, M. Omura, H. Teruya, and A. Thakkar, J. Phys. B **28**, 3113 1995).

[55] F. A. Pahl and N. C. Handy, Mol. Phys. **100**, 3199 2002).

[56] A. Mitin, Phys. Rev. A **6201**, 010501 2000).

[57] See http://physics.nist.gov/PhysRefData/DFTdata/contents.html

[58] B. Bursten and R. Fenske, J. Chem. Phys. **67**, 3138 1977).